

On the origin of X-ray dips in Her X-1

N.I.Shakura¹, M.E. Prokhorov¹, K.A. Postnov² and N.A.Ketsaris¹

¹ Sternberg Astronomical Institute, Moscow University, 119899 Moscow, Russia

² Faculty of Physics, Moscow State University, 119899 Moscow, Russia

Received 23 September 1998, accepted ..., 1998

Abstract. A strong X-ray illumination of the optical star atmosphere in Her X-1, asymmetric because of a partial shadowing by the tilted twisted accretion disk around central neutron star, leads to the formation of matter flows coming out of the orbital plane and crossing the line of sight before entering the disk. We suggest that the absorption of X-ray emission by this flow leads to the formation of pre-eclipse and anomalous dips of type I. These dips are observed during several orbits after turn-on both in the main-on and short-on state. Almost coherent action of tidal torques and matter streams enhances the disk wobbling which causes the disk edge to shield the X-ray source after the turn-on. Anomalous dips of type II and post-eclipse recovery appear due to this process only on the first orbit after turn-on.

Key words: Stars: neutron; stars: individual: Her X-1

1. Introduction

Her X-1 is an accretion-powered 1.24-s X-ray pulsar in a binary system with 1.7-d orbital period (Tananbaum et al. 1972). The source displays 34.85-day X-ray intensity variation due to eclipse by a counter-orbitally precessing tilted accretion disk around the central neutron star (Gerend & Boynton 1976). The X-ray light curve of Her X-1 consists of a main-on X-ray state with a mean duration of ~ 7 orbital periods surrounded by two off-states (also called low-on states) each of ~ 4 orbital cycles, and of a smaller-intensity short-on state with a typical duration of ~ 5 orbits, and is certainly formed by periodic obscurations of the X-ray source by the disk.

As was understood already shortly after the beginning of studies of Her X-1, the accretion disk may be twisted. During the counter-orbital precession of such a disk the outer parts of the disk open the central X-ray source while the inner parts of the disk occult the X-ray source (Boynton 1978). Moreover, a hot rarefied accretion disk corona may exist around its central parts. This makes the ingress to and egress from main-on and short-on states asymmetric. The opening of the X-ray source with a rapid increase

of X-ray intensity is accompanied by a notable spectral changes which evidences for the presence of a strong absorption, whereas the decrease in X-ray intensity occurs more slowly and without appreciable spectral changes (Giaccioni et al. 1973).

One of the intriguing observational facts is that the X-ray source always turns on near orbital phases $\phi_{orb} \simeq 0.2$ or 0.7. Such a behaviour has been explained by Levine & Jernigan (1982) by the accretion disk wobbling twice the orbital period due to tidal torques. Indeed, it is at these orbital phases that the disk angle inclination changes most rapidly.

Another notable feature is that the duration of successive 35-day cycles is as a rule 20, 20.5, or 21 orbital cycles (Staubert et al. 1983). This behaviour has been confirmed by most recent RXTE observations (Shakura et al. 1998).

Even more enigmatic features observed are sudden decreases in X-ray flux (X-ray dips) which are accompanied by significant spectral changes. They have been observed by many X-ray satellites: *UHURU* (Giacconi et al. 1973, Jones & Forman 1976), *Copernicus* and *Ariel V* (Cooke & Page 1975, Davison & Fabian 1977), *Ariel VI* (Ricketts et al. 1982), *OSO-7*, *OSO-8* (Crosa and Boynton 1980), *HEAO-1* (Gorecki et al. 1982), *Tenma* (Ushimaru et al. 1989), *EXOSAT* (Reynolds & Parmar 1995), *Ginga* (Choi et al. 1994; Leahy et al. 1994; Leahy 1997), *RXTE* (Shakura et al. 1998; Scott & Leahy 1998; Kuster et al. 1998). X-ray dips are commonly separated into three groups: pre-eclipse dips (P), which are observed in the first several orbits after X-ray turn-on (up to 7 in main-on and up to 5 in short-on states) and march from the eclipse toward earlier orbital phase in successive orbits; anomalous dips (A), which are observed at $\phi_{orb} \sim 0.45 - 0.65$; post-eclipse recoveries (R), which are occasionally observed as a short delay (up to a few hours) of the egress from X-ray eclipse in the first orbit after turn-on.

Here we suggest a new model for all types of X-ray dips observed in Her X-1. We shall show that the anomalous dips are separated into two types depending on their formation mechanism. The key underlying feature of this model is the anisotropic X-ray heating of the optical star atmosphere produced by the tilted twisted accretion disk.

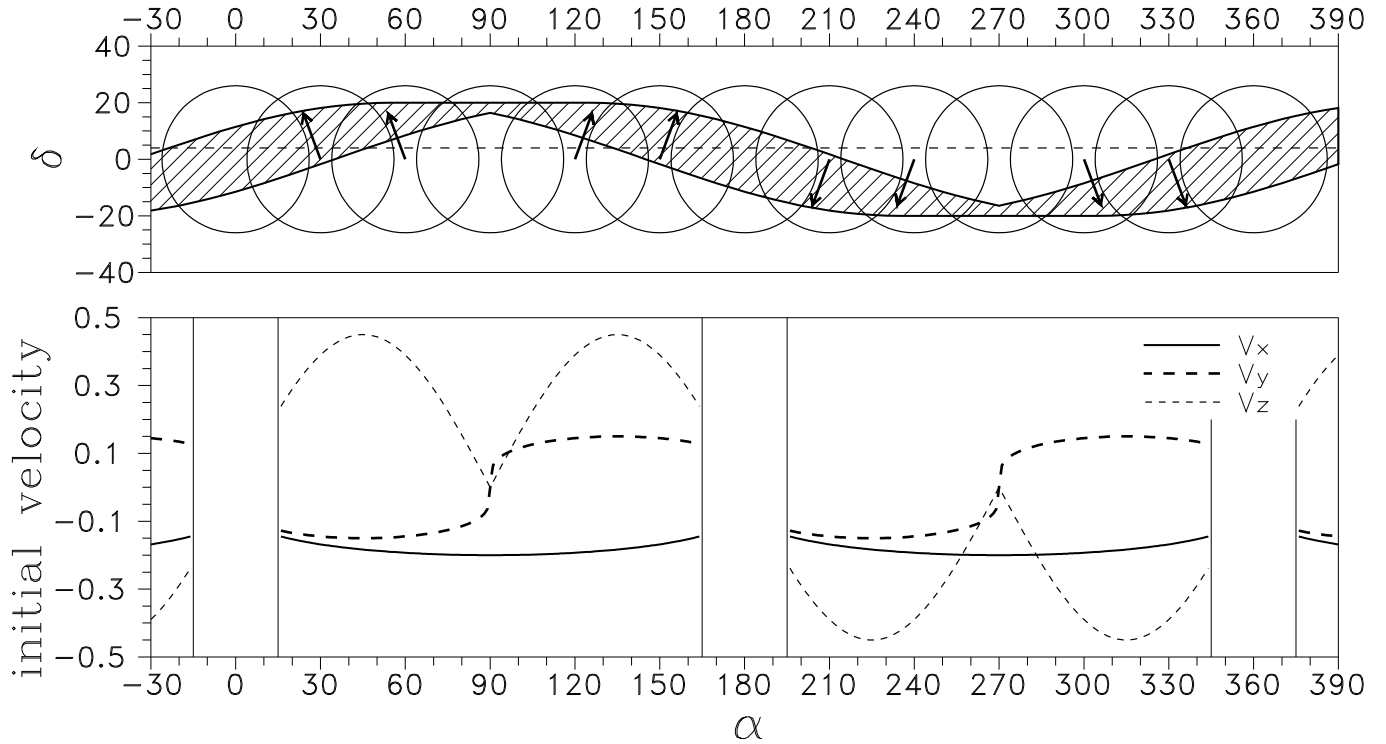


Fig. 1. Upper panel: the passage of HZ Her through the shadow formed by a tilted twisted accretion disk. The coordinates α and δ count from the line of nodes of the middle part of the disk along the orbital motion and from the orbital plane, respectively. The dashed line indicates the position of an observer inclined by $i = 86^\circ$ to the orbit. The arrows show the projection of the initial accretion stream velocity on the plane YZ perpendicular to the orbit. Bottom panel: The initial stream velocity components at the L_1 point in units of the relative orbital velocity 270 km/s. The flows disappear inside the shadow sector between the outer and inner disk node lines.

This leads to the formation of gaseous streams coming out of the orbital plane. Before entering the disk, the streams may cross the observer's line of sight thus producing pre-eclipse and anomalous dips (of type I). Such streams form the outer parts of the accretion disk tilted with respect to the orbital plane. The tidal torques causes the disk to precess in the direction opposite to the orbital motion and also produce a notable wobbling (nutation) motion of the outer parts of the disk twice the synodal period. Due to viscosity the disk becomes twisted and all parts of the disk undergo a notable wobbling caused by both tidal torques and dynamical action of the streams. The X-ray source may be screened for some time from the observer by the outer parts of such a disk in the first orbit after the X-ray turn-on. Type II anomalous dips and post-eclipse recoveries appear in this way.

2. Origin of the pre-eclipse and type I anomalous dips

In our model, a tilted twisted counter-orbitally precessing accretion disk eclipses the central X-ray source between the main-on and short-on states. The outer parts of this

disk is inclined by an angle of $15 - 20^\circ$ relative to the orbital plane. The inner parts of the disk are also tilted by some angle, which can be determined from comparing the durations of low-on states between the main-on and short-on states. As these low-on states are, to an accuracy of 0.5 orbits, of the same duration (4 orbits), the tilt of outer and inner parts of the disk should be comparable.

Such a disk produces an appreciable shadow and the optical star periodically enters this shadow in its orbital motion (Fig. 1). The shadowed region is such that not all the optical star surface is screened by the disk – there always should exist areas illuminated by the X-ray source with a photospheric temperature of 15,000-20,000 K whereas photospheric temperature of the unheated regions is as low as $\sim 8,400$ K. Even higher temperatures (up to 10^6 K) due to soft X-ray absorption by heavy elements are attainable in the chromospheric layers over the photosphere. The X-ray heating of these layers is so strong that NV $\lambda\lambda 1238.8, 1242.8$ doublet with a FWHM of 150 km/s is observed (Boroson et al. 1996).

Such a high temperature induces matter outflow from the optical star which would lie in the orbital plane in the absence of the shadow. The pioneering calculations of such symmetric outflows were carried out in Basko & Sunyaev

(1973). They showed that the induced mass outflow rate and subsequent accretion on the neutron star is sufficient to explain the observed X-ray luminosity $L_x \sim 10^{37}$ erg/s.

When the shadow appears, a powerful pressure gradients emerge in the chromospheric layers near the boundary separating illuminated and obscured parts of the optical star, which initiates large-scale motions of matter near the inner Lagrangian point L_1 with a large velocity component perpendicular to the orbital plane (Arons 1973; Katz 1973). Such a shadow will periodically modulate the matter outflow rate \dot{M} , which is dramatically reduced when the L_1 point is deep inside the shadow, and rises rapidly to a maximum at the moment when the shadow edge intersects the L_1 point. Clearly, the picture repeats twice over the synodal orbital period.

Thus, matter flows non-coplanar with the orbital plane emerge and supply the accretion disk with angular momentum non-parallel to the orbital one. Depending on the initial velocities, these streams may even increase the disk tilt to the orbit. Such streams coming out of the L_1 point intersect the line of sight of the observer at some orbital phases shortly before the X-ray eclipse and shift slowly toward earlier phases as the precession progresses. This is exactly the behaviour of the pre-eclipse X-ray dips observed. The streams intersect the line of sight at other orbital phases as well and thus give rise to the type I anomalous dips.

The problem of matter outflow from an asymmetrically illuminated stellar atmosphere is essentially three-dimensional and requires sophisticated numerical calculations. To obtain the pre-eclipse dips in a simplified model, we calculated non-planar ballistic trajectories of particles ejected from the point L_1 . As a first step, we exploit some trial functions for the initial outflow velocity components outside the shadowed sector (with the optimal width being $\pm 15^\circ$ from the mean disk node line; see Fig. 2 and Table 1). Clearly, the sector lies within the region restricted by the line of nodes of the outer parts of the disk on one side, and by the line of nodes of the inner parts of the disk on the other side. The angle between these lines is 70° (see Table 1).

In a corotating frame with the X-axis directed from the X-ray source to the optical star, the Y-axis pointing along the orbital motion, and the Z-axis perpendicular to the orbital plane, $v_x = -v_x^o |\sin \alpha|^{n_x}$, $v_y = \mp v_y^o |\sin 2\alpha|^{n_y}$, $v_z = \pm v_z^o |\sin 2\alpha|^{n_z}$, with the angle α counted along the orbit from the mean accretion disk node line (Fig. 2). The choice of the sign of $v_{y,z}$ is dictated by the X-ray illumination conditions (see Fig. 1,2). The different angular modulation of velocities comes from the following arguments. The shadow's boundary crosses the L_1 point four times per orbital cycle, so the powerful pressure gradients perpendicular to the shadow's boundary must appear four times per orbital cycle. At the same time, the maximum outflow rate along the X-coordinate is attained when the

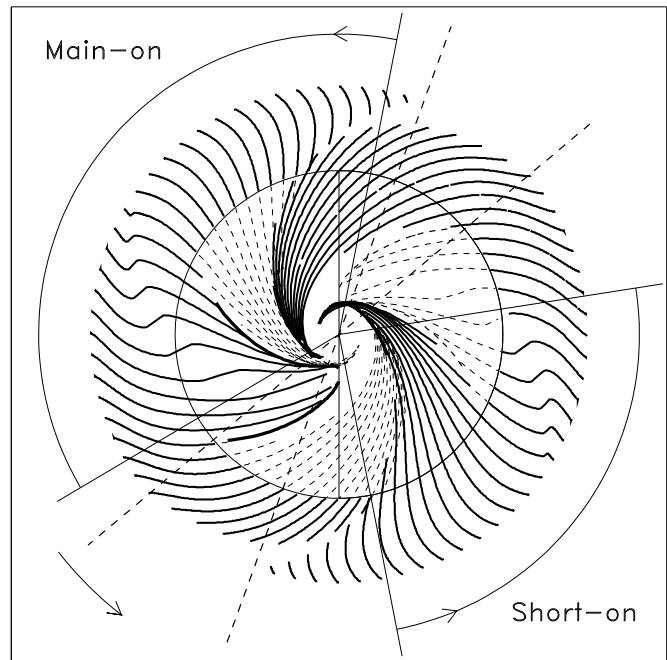


Fig. 2. The projection of the accretion streams onto the orbital plane in the disk reference frame in 5° orbital phase intervals. The orbital motion is counter-clockwise. The central circle indicates the projection of the outer parts of twisted accretion disk intersecting the orbit along the vertical node line, the disk being above the orbit to the right of this line. The inner Lagrangian point is shadowed by the disk within the sector shown by the dashed lines which is restricted by the node lines of the outer and inner parts of the disk. Matter outflow is almost absent inside this cone. The left and right wide sectors shown by solid lines correspond to the main-on and short-on X-ray states, respectively. The thick lines inside the accretion disk show the points where the streams meet the disk plane. The dashed parts of the streams mean they pass under the disk. The observer is above the orbital plane. The bended structure of some stream lines is due to angle modulation of v_z^o velocity component.

irradiation is maximal i.e. when the shadow's boundary is far from the L_1 point, i.e. two times per orbital period.

The initial velocities of particles were taken so that, on the one hand, the dynamical action of the streams on the accretion disk keep it tilted by some angle to the orbit, and on the other hand, the calculated dips occupy the region of the observed dips on $\phi_{orb} - \phi_{pr}$ diagram. We set $\phi_{orb} = 0$ corresponding to the middle of X-ray eclipse and $\phi_{pr} = 0$ at the moment of maximal outer disk opening. On $\phi_{orb} - \phi_{pr}$ diagram, however, it is more convenient to plot ϕ_{pr} in terms of the number of orbital cycles after X-ray turn-on at $\phi_{orb} = 0.75$.

The parameters of the model are summarized in Table 1. Note that with a given disk tilt of 20° and X-ray state durations the binary inclination is unambiguously $i_b =$

86°.0. In principle, the calculations can be done with the disk tilt 15°. Then the binary inclination would be $\approx 87^\circ$. This strict dependence is dictated by the relation between the main-on, short-on, and low-on durations (see Table 1). From independent analyses of optical light curves, the disk radius R_d lies between $\approx (0.2 - 0.3)a$ (Gerend & Boynton 1976, Howarth & Wilson 1983, Shakura et al. 1997). In the present paper we have taken $R_d = 0.3a$.

In a wide range of velocities v_i^0 and parameters n_i the stream crosses the line of sight before the X-ray eclipse and near orbital phases 0.45 – 0.65. We found a good coincidence for the initial velocity components (in units of the orbital velocity $v_{orb} = 2\pi a/P_{orb} \approx 270$ km/s) $v_x^0 \approx 0.2$, $v_z^0 \approx 0.45$, $v_y^0 \approx 0.15$. The calculations were performed for $n_x = n_y = 0.25$, $n_z = 1$. Note that the initial z -component of the stream velocity is about two times higher than its x -component. This is due to large pressure gradients inside the chromosphere near the inner Lagrangian point that appear close to the boundary between the illuminated hot region ($T \sim 10^6$ K) and the shadowed cool region ($T \sim 10^4$ K). We should emphasize that the initial stream velocity does not exceed the sound velocity in the hot region. We also note that small perturbations of the velocity field near L_1 point can result in sizable inhomogeneities of the out-flowing stream, so the pre-eclipse dip formed by such a stream can have a complex structure.

Before colliding with the disk non-planar streams intersect the line connecting the observer and central X-ray source thus absorbing some X-ray flux. We identify these events with the pre-eclipse and type I anomalous dips. In Fig. 3 we plot the calculated and observed dip positions on the $\phi_{orb} - \phi_{pr}$ plane (data from Crosa & Boynton (1980), Ricketts et al. (1982), Shakura et al. (1998)). The contours include the calculated dip positions for different minimal distances between the stream centre and the line of sight (0.02, 0.04, and 0.08). The stream generated when the star again enters the X-ray illuminated sector (see Fig. 2), must also intersect the line of sight during the short-on state $\phi_{pr} \approx 0.25 - 0.55$. This gives rise to the pre-eclipse dips during the short-on state as well, as indeed observed (Jones & Forman 1976; Ricketts et al. 1982; Shakura et al. 1998).

Fig. 3 demonstrates qualitative agreement between the observed and calculated dip positions. Note that in our model parameters additional pre-eclipse X-ray dips can appear at the end of the "main-on" state when the stream from another illuminated sector crosses the line of sight (see Fig. 2,3). It would be interesting to look for these features in detailed X-ray observations. Interestingly, with the parameters assumed, in the first several orbits the pre-eclipse dip is slightly separated from the X-ray eclipse.

Note that a small difference in the calculated and observed anomalous dip positions in the main-on state (Fig. 3) is due to the roughness of the model. The agreement can be made better by shifting the maxima of v_y , v_z velocities by $\sim 10 - 15^\circ$ towards the shadow boundaries.

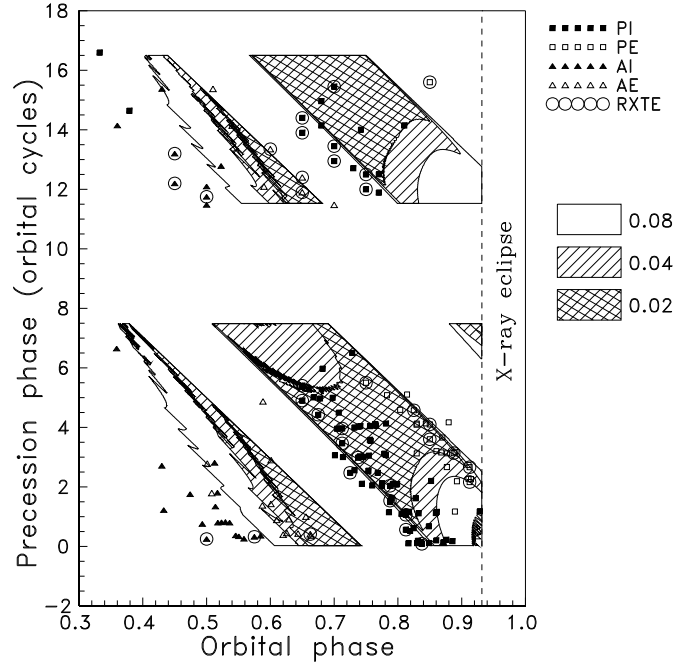


Fig. 3. The part of the plane $\phi_{orb} - \phi_{prec}$ with the observed pre-eclipse and anomalous X-ray dips in the main-on and short-on states. Quadrangles and triangles indicate ingress to (PI) and egress from (PE) the pre-eclipse dips. RXTE data are encircled. The calculated pre-eclipse dips and short anomalous dips arise when the accretion stream intersects the line between the X-ray source and the observer before entering the disk. Different contours correspond to different minimal distances (0.02, 0.04, 0.08) between the stream centre and the line of sight.

For example, one may take gaussian-like trial functions for phase velocity dependence. However, this is hardly worthwhile doing until more detailed X-ray dip observations become available.

3. Features of the precessional motion in Her X-1

The motion of the tilted accretion disk proceeds, on the one hand, under the tidal action from the optical star, and, on the other hand, suffers from the dynamical action of the gaseous streams. The total action of these torques makes it precess with a period of 20.5 orbital cycles (the 35-day X-ray cycle).

First we calculate the tidal torque applied to a ring of matter of radius r at the outer edge of the disk.

$$\frac{d\mathbf{K}_t}{dt} = \int_0^{2\pi} [\mathbf{r} \times \mathbf{f}_t(\phi)] d\phi, \quad (1)$$

where $\mathbf{f}_t(\phi)$ is the tidal force applied to the ring's element. Under the action of this torque the mean counter-orbital precessional motion proceeds and the wobbling at twice the orbital period takes place both in angles α and θ .

Table 1. Model parameters

Binary parameters			
Neutron star mass, M_x		1.4 M_\odot	
Optical star mass, M_o		2.2 M_\odot	
Orbital separation, a		9.1 R_\odot	
Orbital period, P_{orb}		1 ^d .7	
Relative orbital velocity, v_{orb}		270 km/s	
Orbital inclination		86°.0	
X-ray light curve parameters			
Mean precession period, in P_{orb}		20.5	
Main-On duration, in P_{orb}		7.5	
Short-On duration, in P_{orb}		5.0	
Low-On between Main-On and Short-On, in P_{orb}		4	
Low-On between Short-On and Main-On, in P_{orb}		4	
Accretion disk parameters			
Disk radius, R_d		0.3a	
Outer disk radius tilt, θ_o		20°	
§ Inner disk radius tilt, θ_i		20°	
Angle between the line of nodes of inner and outer disk, $\alpha_o - \alpha_i$		+70°	
Accretion stream parameters			
† Initial velocity components at the inner Lagrangian point, in v_{orb}	$v_x = -v_x^o \sin \alpha ^{n_x}$,	$v_x^o = 0.20$,	$n_x = 0.25$
	$v_y = \mp v_y^o \sin 2\alpha ^{n_y}$,	$v_y^o = 0.15$,	$n_y = 0.25$
	$v_z = \pm v_z^o \sin 2\alpha ^{n_z}$,	$v_z^o = 0.45$,	$n_z = 1$
Width of the shadow sectors with no matter outflow, W		±15°	
Position of the shadow sectors bisectrix		$\alpha = 0^\circ, 180^\circ$	
Minimal distances between the stream centre and the line of sight		0.02a, 0.04a, 0.08a	
Resulting disc precession characteristics			
Mean tidal precession rate, $\Delta\alpha_t$		−42°.2 per sidereal orbit	
‡ Mean dynamical precession rate, $\Delta\alpha_d$		+24°.6 per sidereal orbit	

§The difference in the inner and outer disk inclination is determined by the difference between the duration of the low-on states, which are equal to each other to an accuracy of 0.5 orbits.

†The angle α counts along the orbital motion from the mean line of the nodes of the accretion disk.

‡The total precession rate $\Delta\alpha = \Delta\alpha_t + \Delta\alpha_d = -17^\circ.6 \approx 360^\circ/20.5$

3.1. Mean precession rate

We calculated the rate of the mean precessional motion for such a ring and compared it with the well-known analytical expression obtained in quadrupole approximation

$$P_{pr}^t \simeq \Pi_0 \Pi_1 \frac{4}{3} \frac{(q + q^2)^{1/2}}{R_d^{3/2} \cos \theta} P_{orb}, \quad (2)$$

where $q \equiv M_x/M_o \simeq 0.64$ is the mass ratio, $P_{orb} = 1.7^d$ is the orbital period. We introduced here a numerical factor $\Pi_0 < 1$ which can account for the additional effects of higher multiples (see Table 2).

Table 2.

R_d/a	Π_0
0.3	0.87
0.25	0.91
0.2	0.94
0.15	0.97
0.1	0.985

In fact, we deal not with a rigid ring but with a viscous disk in which the inner parts should precess much more slowly under the action of tidal torques. However, due to viscosity the disk precesses as a whole with one period which is slightly larger than the period of the outer parts. To account for this effect, we introduced another numerical factor $\Pi_1 \sim 1.1$. With the assumed parameters of Her X-1 ($q \simeq 0.64$, $R_d \simeq 0.3a$, $\theta \simeq 20^\circ$), the pure tidal precession rate per sidereal orbital period would be $\sim -42^\circ.2$, whereas the observed rate is $-17^\circ.6$. The difference between them is compensated by the dynamical action of the streams.

One can calculate dynamical action of the streams on the disk by solving the equation for the disk angular momentum \mathbf{K}_d change:

$$\frac{d\mathbf{K}_d}{dt} = [\mathbf{r} \times \mathbf{f}] = \dot{M}_{in} [\mathbf{r} \times \mathbf{v}]. \quad (3)$$

where $[\mathbf{r} \times \mathbf{f}]$ is the torque applied to the disk by a stream with mass flow rate \dot{M}_{in} colliding with the disk at velocity \mathbf{v} at a distance \mathbf{r} from the disk centre. The outflow rate is $\dot{M}_{out} \propto |\mathbf{v}|_{L_1}$. Clearly, a phase lag $\Delta\alpha$ exists between the time of outflow of a given portion of matter

from the L_1 point and its encounter with the disk, so $\dot{M}_{in}(\alpha) = \dot{M}_{out}(\alpha + \Delta\alpha)$, which we take into account. Although we cannot take into account the dependence of the accretion rate on the matter density at the Lagrangian point, nevertheless we are able to introduce a dimensionless numerical factor such that the dynamical action of the streams together with the tidal torques lead to the observed precession rate $-17^\circ.6$ per sidereal orbit. Thus the dynamical action makes the disk to precess along with the orbital motion with the rate $-17^\circ.6 - (-42^\circ.2) = +25^\circ.6$ per sidereal orbit. So the absolute value of the contribution of the dynamical torques to the observed precession rate is of order 50% of tidal torques. For a disk with size $0.25a$ the tidal precession rate would be $-30^\circ.7$ and correspondingly to provide the observed rate $-17^\circ.6$ per orbit the dynamical precession rate should be $13^\circ.2$ per orbit, i.e the contribution of dynamical torques would be $\sim 40\%$ of tidal torques. If the disk radius is well defined then the α -parameter of disk accretion can be evaluated by comparison of dynamical and tidal actions.

The streams supplying the disk with angular momentum would change not only its precession rate but also its tilt to the orbit. We found that for fixed v_x^0 , v_y^0 and v_z^0 the streams tend to increase a small disk tilt and *vice versa*, if the tilt is not small, the streams would decrease it, so that an equilibrium disk inclination angle θ can always be found for given v_i^0 . The viscous tidal effects tend to decrease the equilibrium tilt by a factor $\tau_t/(\tau_t + \tau_d)$, where $\tau_d \equiv M_d/\dot{M}$ and τ_t are characteristic times for dynamical and viscous tidal actions, respectively.

Note that with accretion rate \dot{M} growth the dynamical torque increases, while the tidal torque does not change (assuming the constant disk radius). So the net precessional period should increase. Indeed, such a correlation has been deduced between the duration of the 35-day cycle and the mean X-ray flux from analysis of observations by BATSE (Wilson et al. 1994) and RXTE (Shakura et al. 1998).

3.2. Wobbling of the outer disk parts

In addition to the mean precession motion of the disk, there is a wobbling of the outer parts of the disk due to both the tidal torques and dynamical action of the streams. The pure tidal wobbling in quadruple approximation was studied by Levine & Jernigan (1982) who showed that this effect causes the source to turn-on near the orbital phases 0.2 and 0.7.

When calculating the tidal wobbling we used the general Eq.(1). Then we approximated the wobbling motion of the outer disk by the following harmonic functions: for the angle of the line of nodes of outer disk

$$\Delta\alpha_t \equiv \alpha_o - \langle\alpha_o\rangle = A_2 \sin 2\alpha_o,$$

for the tilt of the outer disk

$$\Delta\theta_t \equiv \theta_o - \langle\theta_o\rangle = B_2 \cos 2\alpha_o.$$

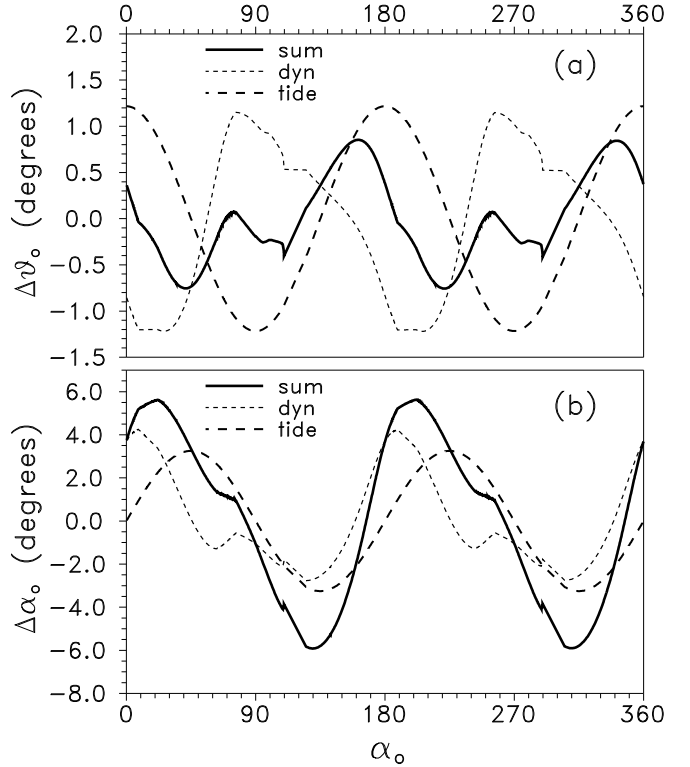


Fig. 4. The wobbling variations of the outer disk tilt $\Delta\theta_o$ (a) and its line of nodes $\Delta\alpha_o$ (b) as a function of the phase angle α_o .

Higher-order multiples contribute less than about 1%, i.e. the tidal wobbling follows almost exactly a pure sine law at the double orbital frequency, while the quadruple approximation for the mean precession motion turns out to be more crude (see Table 2).

We also calculated numerically the wobbling due to dynamical action of the stream with taking into account the renormalization of the dynamical torques to the observed precession rate per orbit discussed above. Since the stream torque depends on the orbital phase in a complex way (unlike the tidal torque, it is far from being sine-like), the resulting periodical variations of $\Delta\alpha_o$ and $\Delta\theta_o$ with the orbital phase have very complex shapes (see Fig. 4). In Fig. 4(a), we have plotted the tidal, dynamical, and the total change in the outer disk tilt $\Delta\theta_o$ as a function of the phase angle of the mean line of nodes of the outer disk α_o . Fig. 4(b) shows the same for the wobbling of the line of nodes of the outer disk $\Delta\alpha_o$.

To conclude this section, we note that in a general case the accretion rate \dot{M} (and hence dynamical torques applied to the disk) may be phase-dependent in addition to dependence through the stream velocity $\mathbf{v}(\alpha)$: $\dot{M}_{out} \propto |\mathbf{v}|f(2\alpha)$, where f is some periodical function. This additional dependence has been neglected in our calculations ($f \equiv 1$).

4. Origin of post-eclipse recoveries and type II anomalous X-ray dips

Unlike the pre-eclipse dips and type I anomalous dips, the anomalous dips of type II and post-eclipse recoveries are formed by another mechanism. The vector of the disk angular momentum moves along a precession cone and undergoes an oscillating (wobbling) motion twice the synodical orbital period.

We recall that the secular precession effects due to dynamical and tidal interactions have the opposite signs. As shown above, the oscillating part of both torques behaves in a more complex way. So does the angle ϵ between the line of sight and the outer disk plane:

$$\cos \epsilon = \cos i \cos \theta_o + \sin i \sin \theta_o \cos \phi_{pr}. \quad (4)$$

At the precession phases where the outer disk is observed face-on, the variation in ϵ is mostly due to changes in the angle θ_o , which are small. As seen from Fig.4(a), the deviations of angle θ_o caused by tidal and dynamical actions are in counter-phase and practically compensate for each other. In contrast, when the disk is observed edge-on, the main contribution into change of ϵ comes from the variations of α_o , for which the dynamical and tidal torques act almost coherently (Fig. 4(b)) enhancing the resulting change in ϵ .

Fig. 5 shows the angle ϵ between the line of sight and the outer disk plane (the jagged curve). As seen from this figure, X-ray turn-ons may be followed by a short time interval in which the X-rays are again occulted by the outer edge of the disk. We identify this effect with either a type II anomalous dip (A) at $\phi_{orb} \sim 0.4 - 0.6$) or a post-eclipse recovery (R) at $\phi_{orb} \simeq 0.1 - 0.2$. We also note that these features do not appear more than in one orbital cycle after turn-on and moreover, unless the disk radius is unrealistically large ($> 0.3a$), only a post-eclipse recovery or an anomalous dip of type II is observed.

5. Discussion

We have suggested a model explaining absorption features (X-ray dips and post-eclipse recoveries) in the X-ray curve of Her X-1. In this model, anisotropic X-ray heating of the optical star atmosphere causes the matter outflow from the inner Lagrangian point to proceed in the form of non-coplanar streams. These streams intersect the line of sight of the observer forming different absorption features (X-ray dips). The model demonstrates a satisfactory agreement with observed positions of these features on $\phi_{orb} - \phi_{pr}$ plane. The agreement can be made better by choosing trial functions for the initial stream velocity components at the inner Lagrangian points in a Gaussian-like form.

The X-ray observations of Her X-1 from *EXOSAT* (Reynolds and Parmar 1995) and especially from *Ginga* (Choi et al. 1994; Leahy et al. 1994; Leahy 1997) satellites

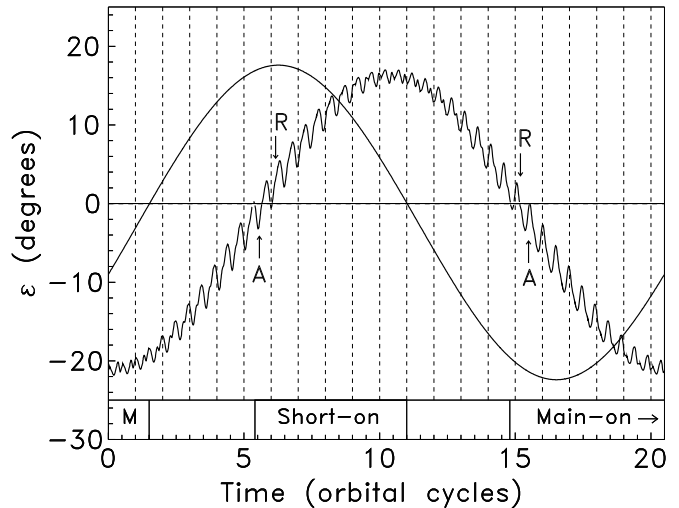


Fig. 5. The angle ϵ between the line of sight and the outer accretion disk plane (the jagged line) and inner accretion disk plane (the smooth line) as a function of time (in orbital cycles). The small vertical arrows indicate the anomalous X-ray dips of type II (A) and post-eclipse recovery (R).

revealed that the absorption dips have different duration and complex structure. In our model, we expect the pre-eclipse X-ray dips and type I anomalous dips which are formed due to absorption in the streams to have a complicated structure, while the type II anomalous dips and post-eclipse recoveries, which are due to the outer disk wobbling, must be more smooth. So the observation of energy distribution inside dips would be very important and dedicated continuous X-ray observations covering the whole 35-day cycle are highly desirable to clarify this picture.

The essential feature of our model is the presence of a twisted tilted accretion disk around the central neutron star. The presence of such a disk in Her X-1 binary has long been discussed in literature (Petterson 1977, Schandl & Meyer 1994, see detailed reference in Wijers & Pringle 1998). We used a twisted disk in which the outer parts are tilted to the orbit by the same amount as the inner parts. The calculation made by Wijers & Pringle (1998) have suggested that the inner parts of the disk may even have a higher tilt than the outer parts by the action of radiation pressure. When calculating the twisted disk parameters ($\theta_o, \theta_i, \alpha_o - \alpha_i$) we have come from the observed duration of the main-on (7.5 orbits), short-on (5 orbits), and low-on (4+4 orbits) states in Her X-1. As the error in the determination of these states may be noticeable (about 0.5 orbits), it is not excluded that the inner parts of the disk may be much more tilted to the orbit. For instance, if the durations of these states were related as 7 (main-on) : 4.5 (1st low-on) : 5.5 (short-on) : 3.5 (2d low-on), the inner disk tilt would be $\sim 60^\circ$ with the twist angle $\alpha_o - \alpha_i \sim 90^\circ$. In our model of twisted accretion disk the twist angle

could be so high that the "windows" where main-on and short-on states are observed may be "closed" (see Fig. 5). This can explain the prolonged off-state observed during 9 months in 1983-1984 (Parmar et al. 1985).

A geometrical thick accretion disk with $H/R \sim 0.2$ would generally produce a similar shadow on the optical star atmosphere as the twisted geometrically thin disk. Since in our model it is the shape of the shadow that determines the initial velocity components, the behaviour of X-ray dips can be explained by such a thick disk as well. But we do use the thin twisted disk models because a very high temperature is required to produce such a thick disk. Clearly, the choice of the disk model requires additional studies and cannot be uniquely made solely on the grounds of X-ray dip behaviour. In principle, a more thorough study of the optical light curves of HZ Her could put new bounds on the disk parameters.

Acknowledgements. We thank the referee Dr. Susanne Schandl for constructive notes. The work was supported by the Grant "Universities of Russia", No5559, Russian Fund for Basic Research through Grant No 98-02-16801 and the INTAS Grant No 93-3364-ext. N.I.S. acknowledge the staff of Cosmic Radiation Laboratory of RIKEN (Tokyo) and Max-Planck Institut für Astrophysik (Garching) for hospitality.

References

- Arons, J., 1973, ApJ 184, 539
 Basko, M.M. & Sunyaev, R.A., 1973, ApSS 23, 117
 Boroson, B., Vrtilik, S.D., McCray, R., Kallman, T., & Nagase, F., 1996, ApJ 473, 1079
 Boynton, P.E., 1978, in: Physics and Astrophysics of Neutron Stars and Black Holes, Eds. R. Giacconi, R. Ruffini, Soc. Ital. di Fisica, Bologna, p. 111
 Choi, C.S., Nagase, F., Makino, F., Dotani, T., & Min, K.W., 1994, ApJ 422, 799
 Cooke, B.A., & Page, C.G., 1975, Nat. Phys. Sci. 256, 712
 Crosa, L., & Boynton, P.E., 1980, ApJ 235, 999
 Davison, P.J.N., & Fabian, A.C., 1977, MNRAS 178, 1p
 Gerend, D., & Boynton, P.E., 1976, ApJ 209, 562
 Giacconi, R., Gursky, H., Kellogg, E., et al., 1973, ApJ 184, 227
 Gorecki, A., Levine, A., & Bautz, M., et al., 1982, ApJ 256, 234
 Howarth, I.D., & Wilson, R., 1983, MNRAS 202, 347
 Jones, C., & Forman, W., 1976, ApJ 209, L131
 Katz, J.I., 1973, Nat. Phys. Sci. 246, 87
 Kuster, M., Wilms, J., Blum, S., et al., 1998, in Proc. 3d INTEGRAL Workshop, eds. A. Bazzano, S. Di Cosimo, in press.
 Leahy, D.A., 1997, MNRAS 287, 622
 Leahy, D.A., Yoshida, A., & Matsuoka, M., 1994, ApJ 434, 341
 Levine, A.M., & Jernigan, J.G., 1982, ApJ 262, 294
 Parmar, A.N., Pietsch, W., McKechnie, S., et al., 1985, Nat. 313, 119
 Petterson, J., 1977, ApJ 218, 783
 Ricketts, M.J., Stanger, V., & Page, C.G., 1982, in: Accreting Neutron Stars, eds. W. Brinkmann, J. Trümper, ISO, Garching bei München, p. 100
 Reynolds, A.P., & Parmar, A.N., 1995, A&A 297, 747
 Schandl, S., & Meyer, F., 1994, A&A 289, 149
 Scott, D.M., & Leahy, D.A., 1998, preprint astro-ph/9809152
 Shakura, N.I., Smirnov, A.V., & Ketsaris, N.A., 1997, in: Accretion Phenomena and Related Outflows, eds. D.T. Wickramasinghe, G.V. Bicknell, L. Ferrario, Astron. Soc. Pacif., San Francisco, p. 379
 Shakura, N.I., Ketsaris, N.A., Prokhorov, M.E., & Postnov, K.A., 1998, MNRAS 300, 992
 Staubert, R., Bezler, M., & Kendziorra, E., 1983, A&A 117, 215
 Tananbaum, H., Gursky, H., Kellogg, E.M., et al., 1972, ApJ 174, L143
 Ushimaru, N., Tawara, Yu., Koyama, K., et al., 1989, PASJ 41, 441
 Wijers, R.A.M.J., & Pringle, J.E. 1998, preprint astro-ph/9811056
 Wilson, R.B., Finger, M.H., Pendelton, G.N., Briggs, M., & Bildsten, L., 1994, in: The Evolution of X-ray Binaries, eds. S.S. Holt, C.S. Day, AIP, New York, p. 475